Search for two-phonon gamma vibrational states in ^{164}Dy

D. F. Winchell,* I. Y. Lee,† C. Baktash, J. D. Garrett, M. L. Halbert, N. R. Johnson, and F. K. McGowan
Physics Division, Oak Ridge National Laboratory, Oak Ridge, Tennessee 37831

C. H. Yu‡
Physics Department, University of Tennessee, Knoxville, Tennessee 37996
(Received 7 December 1994)

Excited states in ^{164}Dy were produced using Coulomb excitation. Rotational properties of the ground-state and gamma-vibrational band were studied. Angular distribution and band-mixing parameters were extracted from the data. No evidence was found for a two-phonon gamma vibration with anharmonicity in the range $1.7 \leq E(4^+_{\gamma\gamma})/E(2^+_\gamma) \leq 2.7$.

PACS number(s): 21.10.Re, 21.60.Ev, 23.20.−g, 27.70.+q

I. INTRODUCTION

Rotation and vibration are the two important low energy collective excitations in nuclei. Rotational motion has been extensively studied in recent decades in both theoretical and experimental works. The rotational alignment of the single particle angular momentum, a result of the interplay of the rotational with the single-particle motion, has been the most extensively studied subject in high-spin spectroscopy. Vibrational excitations, however, are not as well understood as rotational motion. The interaction of the vibration with the single-particle motion is expected to produce anharmonicities which cause the shifting and splitting of the multiphonon levels and the deviation of the transition matrix element from the harmonic values. Therefore, the study of the multiphonon states can provide information on the interaction between the vibrational and single-particle degrees of freedom.

The one-phonon gamma vibrational states are well known experimentally in the deformed rare-earth region [1]. They tend to have excitation energies in the range 700–1500 keV. The lowest energies occur near ^{164}Dy and ^{188}Os, and these can be understood in terms of the existence near the Fermi level of orbitals which can be coupled by the r^2Y_{22} operator associated with gamma vibration. In most cases, the $E2$ matrix elements between the ground state and the one-phonon states have been measured [2]. The values of these matrix elements indicate a collectivity of about ten times that of the single-particle values. Very little is known about the behavior of vibrational states at high rotational frequency, due to the fact that these states are not strongly populated in fusion reactions commonly used for high-spin studies. Coulomb excitation can populate these states and provide information on the rotation-vibration interaction at high rotational frequencies. Various theoretical approaches have been used to characterize possible two-phonon vibrational states in deformed nuclei. Using the quasiparticle-phonon nuclear model, Soloviev [3] concluded that such states could not exist due to Pauli blocking effects which push the two-phonon states upward in energy to 3–4 MeV, where the wave functions become fragmented. Piepenbring and Jammari [4] used the multiphonon method (MPM) to predict that the 4^+ two-phonon gamma vibrational state lies at about 2.6 times the one-phonon excitation energy in ^{168}Er, with a transition strength to the one-phonon band comparable to the one-phonon to ground-band strength. In a subsequent paper [5], it was found that the same conclusions regarding anharmonicity and collectivity apply to other deformed nuclei, including ^{164}Dy.

Several attempts have been made in recent years to identify two-phonon vibrational states in rare-earth nuclei. It is of particular importance to measure transition quadrupole moments, since it is possible for 4^+ states of a single-particle nature to decay to gamma-vibrational states [6]. Using a neutron-capture reaction and a curved-crystal gamma-ray spectrometer, Davidson *et al.* [7] identified all levels in ^{168}Er up to an excitation energy of 2.5 MeV. A $K^\pi = 4^+$ band with a 4^+ level at 2055 keV and a 5^+ level at 2169 keV was observed. The identification of this 4^+ state in ^{168}Er as a two-phonon gamma vibration was recently made [8] using the gamma-ray-induced Doppler-broadening technique to determine the $B(E2)$ values for the 4^+ and 5^+ states. The values obtained indicate a large degree of collectivity and are in good agreement with theories which treat the 4^+ state as a two-phonon structure, such as the MPM. The anharmonicity ratio, $R(4) = E(4^+_{\gamma\gamma})/E(2^+_\gamma)$ is found to be 2.5 for ^{168}Er, close to the MPM prediction. Oshima and co-workers [9] have investigated this state using Coulomb excitation, and have also identified two two-phonon states in ^{194}Os. A 4^+ state at energy

*Present address: Department of Physics and Astronomy, University of Pittsburgh, Pittsburgh, PA 15260.
†Present address: Lawrence Berkeley Laboratory, University of California, Berkeley, CA 94720.
‡Present address: Nuclear Structure Lab, University of Rochester, Rochester, NY 14627.

1646 keV in the nucleus ^{154}Gd has also recently been identified as a two-phonon state [10], on the basis of decay intensities. The anharmonicity ratio in this case is 1.7, somewhat smaller than the ratio for ^{168}Er. At higher mass, Korten *et al.* [11] have identified a rotational band built on a nearly harmonic two-phonon vibration in the deformed nucleus ^{232}Th. Given these recent experimental successes, it seemed reasonable to search for a two-phonon state in ^{164}Dy.

II. EXPERIMENTAL PROCEDURE

In order to maximize the likelihood of detecting two-phonon vibrational states in a Coulomb excitation reaction, gammas were detected in coincidence with backscattered beam particles. The beam, energy, and angle of the particle detectors were chosen to maximize the yield of vibrational states with respect to ground-band states, based on the results of calculations using the Winther-deBoer Coulomb excitation program [12].

The experiment was performed at the Holifield Heavy-Ion Research Facility (HHIRF) at Oak Ridge National Laboratory. Excited states in ^{164}Dy were populated using Coulomb excitation induced with a 250 MeV ^{58}Ni beam from the HHIRF tandem. Heavier beams were not used because they would have excited the ground-state band to higher spins, complicating the identification of transitions involving vibrational states. The self-supporting ^{164}Dy target had a thickness of 0.91 mg/cm^2. Gammas were detected with an array of 18 Compton-supressed high-purity germanium (HPGe) detectors and 52 NaI elements of the spin spectrometer. Backscattered beam particles were detected with an array of six surface-barrier silicon detectors centered at 150° with respect to the beam in the laboratory frame and located 32 mm from the target. Total coverage of the Si detectors was 7% of 4π.

Events were defined by the firing of one silicon detector in coincidence with at least one germanium detector. Energy and timing information of these detectors and any other detectors, such as an NaI detector from the spin spectrometer fired in coincidence, were stored in event-by-event mode on tape. Approximately 150 million events were recorded, including 1.2 million in which two or more germanium detectors fired. Energy calibration of the germanium detectors was carried out with ^{88}Y, ^{207}Bi, ^{75}Se, and ^{152}Eu sources. The ^{152}Eu source was also used for relative efficiency calibration of the germanium detectors. The NaI detectors were calibrated using the ^{88}Y, ^{207}Bi, and ^{75}Se sources. Detailed Doppler-shift correction of the gamma energy was made for each event based on the recoil velocity and the angle between the recoiling nucleus and the emitted gamma. The angle and speed of the recoiling nucleus were derived from the angle and energy of the backscattered ^{58}Ni.

III. RESULTS

The combination of the clean reaction and detailed Doppler-shift correction allowed the creation of exceptionally clean spectra. The gamma-gamma coincidence data were sorted into a symmetrized two-dimensional (2D) matrix. A projection of the $E_\gamma - E_\gamma$ matrix is shown in Fig. 1. Along with transitions within the ground-state band and transitions between the gamma-vibrational and ground-state bands in ^{164}Dy, several transitions from the nucleus ^{163}Dy are visible. These were the result of target impurities. A number of previously unobserved transitions were observed in coincidence with known ^{164}Dy lines, and it was possible to assign several new levels to both the ground-state band and the gamma-vibrational band. Assignments were made on the basis of coincidence data and, when possible, angular distribution information from the particle-gamma data. As an example of the quality of the coincidence data, a spectrum created by gating on the $14^+ \rightarrow 12^+$ ground-state band transition is shown in Fig. 2. Lines at 597, 644, and 542 keV are clearly visible. Two fairly strong transitions at 981 and 988 keV were observed and appear to feed into the ground-state band at or above the 8^+ level, but we were unable to make a definite placement in the level scheme. A partial decay scheme, including new states in the ground-state and gamma-vibrational bands in ^{164}Dy,

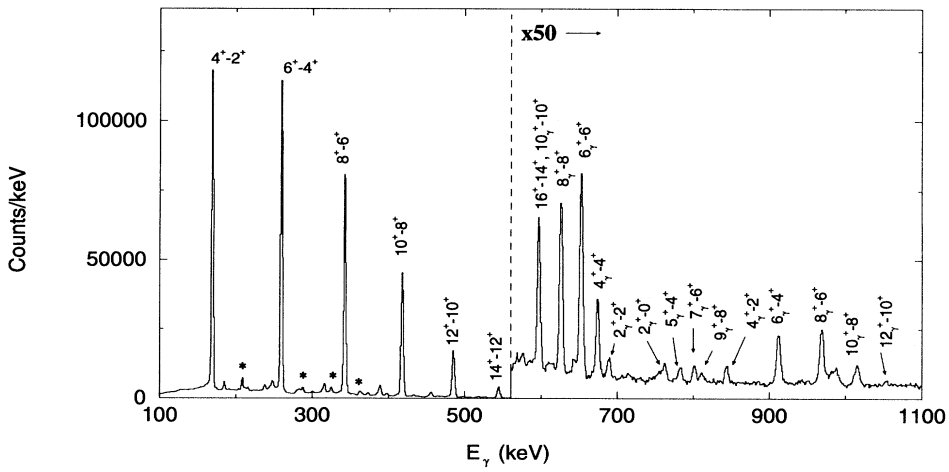

FIG. 1. Spectrum showing the total projection of the two-dimensional $E_\gamma - E_\gamma$ coincidence matrix. Asterisks mark the positions of the most strongly populated transitions in the contaminant nucleus ^{163}Dy.

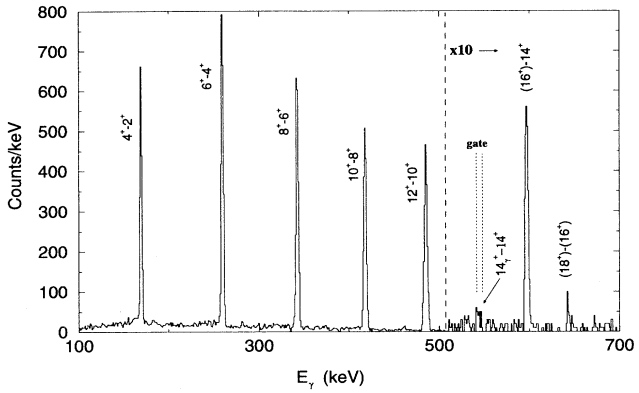

FIG. 2. A spectrum obtained by gating on the $14^+ \rightarrow 12^+$ transition in the ground-state band. The two higher-lying ground-state-band transitions are clearly visible, as is the 542 keV $14^+_\gamma \rightarrow 14^+$ transition.

is shown in Fig. 3. Previous workers [13–18] have reported measurements on the ground-state band to $I = 14$ and the vibrational band to $I = 8$. In a recent progress report [19], Oshima and coworkers report having seen the ground-state band to a spin of 18 and the gamma-vibrational band to a spin of 12, but no level scheme was given.

From our particle-gamma data it was possible to extract angular distribution information for all but the lowest of the in-band ground-state band transitions, for most of the interband transitions between the gamma and ground-state bands, and for most of the in-band gamma-band transitions between states with even spin. The transitions with energy 154.5, 518, 542, 568, 1053, and 1086 keV were too weak to resolve in the ungated spectra. It is assumed that most of the strength of the 597 keV doublet belongs to the $(16^+) \rightarrow 14^+$ ground-state band transition. The 18 HPGe detectors were placed at six angles with respect to the beam direction. For the purposes of determining angular distributions, two pairs of angles symmetric about 90° were identical, leaving four data points for each fit. An example of the angular distribution analysis is given in Fig. 4, where the data and least-squares fit for the 626 keV, $8^+_\gamma \rightarrow 8^+$ transition are shown. Intensities and angular distribution parameters are listed in Table I. Mixing ratios, $\delta = \langle|M(E2)|\rangle/\langle|M(M1)|\rangle$, for the $I \rightarrow I$ and $I \rightarrow I-1$ transitions between the gamma and ground-state bands were extracted and are listed in Table II, along with results from previous experiments. The phase convention of Rose and Brink [20] was used. As an example of the analysis used to extract mixing ratios, Fig. 5 shows the χ^2 vs $\tan^{-1}(\delta)$ plot used to determine the mixing ratio for the $8^+_\gamma \rightarrow 8^+$ transition. Within uncertainties, our results are in agreement with those reported by Hooper *et al.* [15], except in the case of the $2^+_\gamma \rightarrow 2^+$ transition where we obtain the opposite sign.

Using branching ratio data it is possible to extract information regarding the mixing of the ground-state and

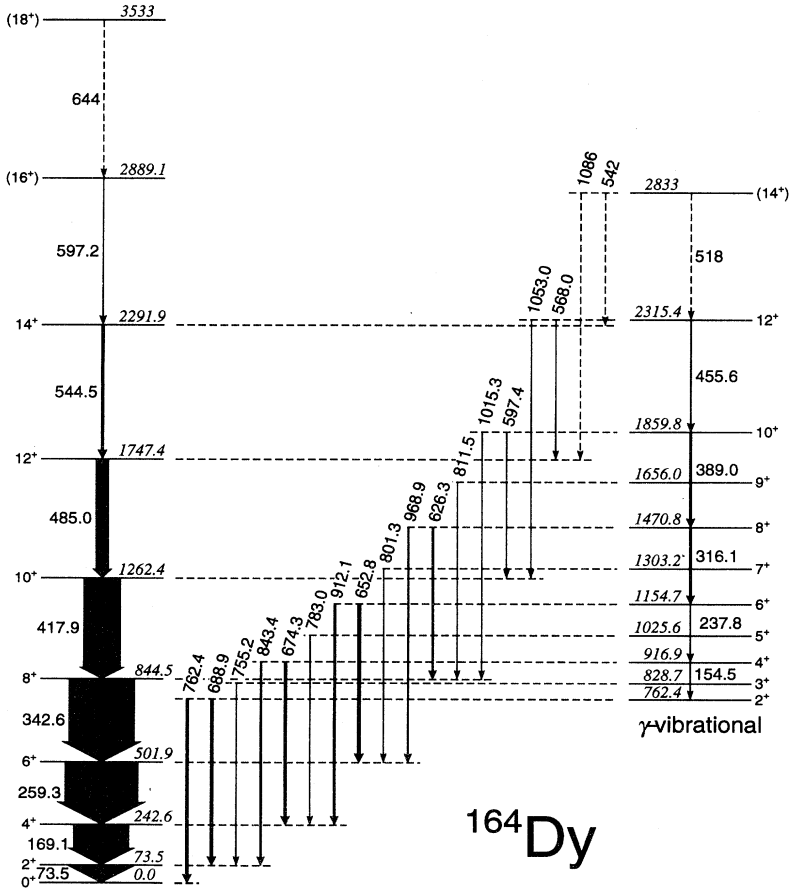

FIG. 3. A partial decay scheme for ^{164}Dy showing the ground-state and gamma-vibrational bands. The widths of the transition arrows are proportional to the observed intensity.

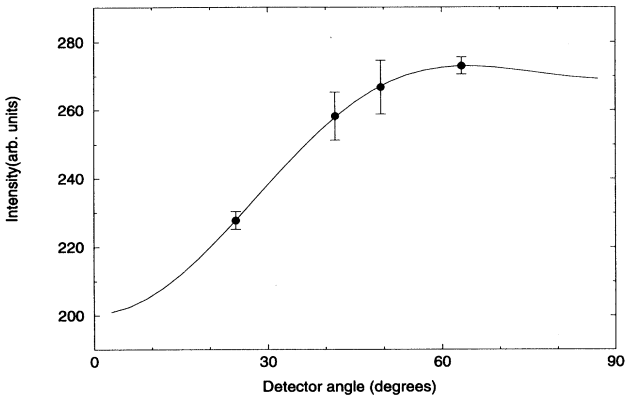

FIG. 4. The angular distribution data and fit for the 626.3 keV $8^+_\gamma \rightarrow 8^+$ transition.

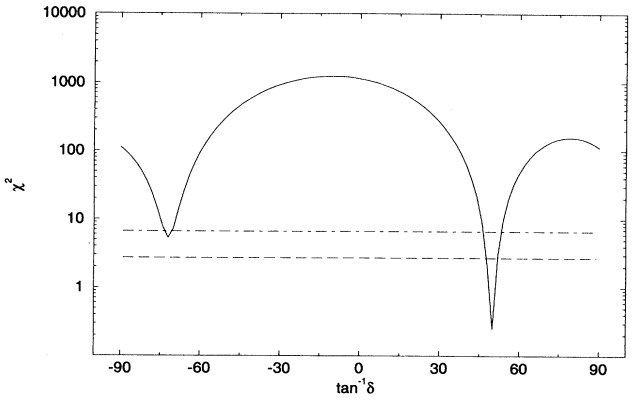

FIG. 5. A plot of χ^2 vs $\tan^{-1}\delta$ for the $8^+_\gamma \rightarrow 8^+$ transition, used to determine the mixing ratio δ. The dashed and dot-dashed lines represent the 10% and 1% confidence levels, respectively.

TABLE I. Relative intensities and angular distribution coefficients for gamma rays observed in this work. Intensities are not corrected for internal conversion.

E_γ (keV)	I_i^π	I_f^π	Intensity[a]	a_2	a_4
169.1	4^+	2^+	100 (2)	0.08 (3)	0.15 (5)
259.3	6^+	4^+	132 (2)	0.16 (3)	0.07 (5)
342.6	8^+	6^+	118 (1)	0.22 (2)	0.01 (3)
417.9	10^+	8^+	67 (1)	0.29 (2)	-0.05 (3)
485.0	12^+	10^+	23.7 (3)	0.35 (2)	-0.06 (4)
544.5	14^+	12^+	5.6 (1)	0.35 (2)	-0.10 (4)
597.2	$(16)^+$	14^+	1.89 (11)	0.08 (4)	-0.07 (7)
644	$(18)^+$	$(16)^+$	0.20 (2)	0.17 (18)	-0.03 (35)
762.4	2^+_γ	0^+	5.6 (1)	0.32 (2)	-0.32 (4)
688.9	2^+_γ	2^+	5.8 (1)	0.00 (2)	-0.14 (4)
755.2	3^+_γ	2^+	0.66 (2)	0.10 (6)	0.16 (11)
843.4	4^+_γ	2^+	3.4 (1)	0.31 (3)	-0.13 (5)
674.3	4^+_γ	4^+	5.5 (1)	-0.09 (2)	-0.10 (4)
783.0	5^+_γ	4^+	0.55 (2)	0.14 (6)	-0.20 (11)
912.1	6^+_γ	4^+	4.1 (1)	0.22 (3)	-0.01 (5)
652.8	6^+_γ	6^+	6.4 (1)	-0.09 (2)	-0.10 (4)
801.3	7^+_γ	6^+	0.43 (2)	0.18 (7)	-0.22 (13)
968.9	8^+_γ	6^+	2.9 (5)	0.18 (3)	0.07 (5)
626.3	8^+_γ	8^+	3.8 (5)	-0.13 (4)	-0.10 (5)
811.5	9^+_γ	8^+	0.20 (1)	0.05 (13)	0.41 (24)
1015	10^+_γ	8^+	0.80 (2)	0.30 (6)	-0.33 (11)
237.8	6^+_γ	4^+_γ	1.8 (3)	0.14 (28)	0.08 (54)
316.1	8^+_γ	6^+_γ	4.8 (1)	0.10 (5)	0.27 (8)
389.0	10^+_γ	8^+_γ	4.9 (1)	0.16 (4)	0.14 (7)
455.6	12^+_γ	10^+_γ	2.7 (1)	-0.05 (4)	0.14 (8)
981	–[b]	–[b]	0.52 (2)	-0.58 (7)	0.61 (14)
988	–[b]	–[b]	0.66 (2)	-0.28 (7)	-0.09 (13)

[a]Normalized to $4^+ \rightarrow 2^+$ transition.
[b]Transition not placed in level scheme.

TABLE II. Mixing ratio δ from this work and previous work.

Transition	This work	Ref. [15]
$2^+_\gamma \rightarrow 2^+$	$-9.5^{+0.8}_{-1.0}$	$5.7^{+\infty}_{-3.6}$ $0.67^{+0.52}_{-0.35}$
$4^+_\gamma \rightarrow 4^+$	$-6.6^{+0.8}_{-1.1}$	$-2.7^{+1.3}_{-8.7}$ $0.48^{+0.36}_{-0.27}$
$8^+_\gamma \rightarrow 8^+$	1.18±0.05	
$3^+_\gamma \rightarrow 2^+$	-0.29±0.05	-0.23±0.13 $28.6^{+\infty}_{-22.3}$
$5^+_\gamma \rightarrow 4^+$	-0.19±0.06	$-0.36^{+0.22}_{-0.26}$ $-5.1^{+2.8}_{-\infty}$
$7^+_\gamma \rightarrow 6^+$	$-0.21^{+0.08}_{-0.09}$	
$9^+_\gamma \rightarrow 8^+$	$-0.32^{+0.15}_{-0.21}$ $-9.5^{+6.0}_{-\infty}$	

gamma-vibrational bands [21,22]. The band-mixing parameter Z_γ is proportional to the mixing amplitude between the ground-band and gamma-band wave functions, and can be extracted from the data using the relationships

$$B(E2; I \rightarrow I) = B_0(E2; I \rightarrow I)(1 + 2Z_\gamma)^2 \quad (1)$$

and

$$B(E2; I \rightarrow I-2) = B_0(E2; I \rightarrow I-2) \times (1 - (2I-3)Z_\gamma)^2, \quad (2)$$

where $B_0(E2)$ is the unperturbed (Alaga) strength, and the transitions are presumed to be between the gamma and ground-state bands. Table III gives the branching ratios and extracted Z_γ's for the decays from the even-spin part of the gamma band to the ground-state band. The weighted average of the four experimental values of Z_γ is 0.033, consistent with all of the experimental values to within uncertainties. This average is slightly smaller than the value of about 0.05 previously obtained [13] from the deexcitation of the 2^+_γ and 4^+_γ states.

TABLE III. Branching ratios and extracted band-mixing parameters for gamma-band to ground-state-band transitions in ^{164}Dy.

	$B(E2; I \rightarrow I)/B(E2; I \rightarrow I-2)$		
I_i	Experiment	Rotational (Alaga)	Z_γ
2	1.72(4)	1.43	0.031(5)
4	4.95(17)	2.93	0.035(3)
6	8.31(24)	3.71	0.032(2)
8	11.6(25)	4.18	0.028(10)

IV. DISCUSSION

A. Rotational characteristics

Both the gamma-vibrational band and the ground-state band can be examined within the framework of the cranking model. The aligned angular momentum, i_x, was calculated using a reference based on the lowest six transitions in the ground-state band, which gives values of $\mathcal{J}_0 = 40.6$ and $\mathcal{J}_1 = 114.2$ for the Harris parameters. In Fig. 6, i_x is plotted as a function of $\hbar\omega$ for the ground-state and gamma bands. The yrast band is clearly undergoing an alignment at $\hbar\omega = 300$ keV, probably a neutron [633]7/2 two-quasiparticle excitation [23]. The gamma-vibrational band steadily increases in alignment from about 0.4 $\hbar$ to 1.1 $\hbar$. Calculations by Bès *et al.* [24] show the wave function of the gamma-vibrational state to be composed primarily of $\nu([523]5/2^- \otimes [521]1/2^-)$, $\nu([521]1/2^- \otimes [521]3/2^-)$, and $\pi([411]3/2^+ \otimes [411]1/2^+)$ two-quasiparticle excitations. While the band mixing parameter is essentially constant, as discussed above, Fig. 6 indicates that as rotational frequency increases, the wave functions of the states in the gamma-vibrational band favor more rotation-aligned configurations.

B. Two-phonon states

In an attempt to observe a possible transition between a two-phonon gamma vibrational state and the one-phonon 2^+ state at 762 keV, spectra were created by placing gates on the 762 keV $2^+_\gamma \rightarrow 0^+$ transition and 689 keV $2^+_\gamma \rightarrow 2^+$ transition in the gamma-gamma coincidence data. The sum of these spectra is shown in Fig. 7 for the energy range 500 to 1630 keV. A $4^+_{\gamma\gamma} \rightarrow 2^+_\gamma$ transition in this region would correspond to an excitation of 1.7 to 3.1 times the single-phonon excitation energy. The broad structure between 1330 and 1600 keV is due to coincidence with the $2^+ \rightarrow 0^+$ transition in ^{58}Ni. At energies below 1330 keV there is only one peak standing out from the statistical fluctuations of the background,

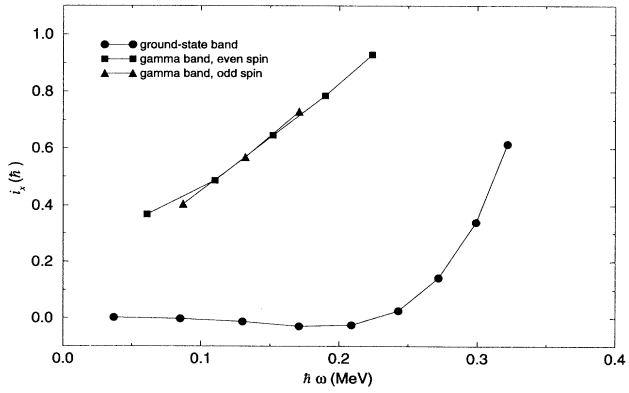

FIG. 6. Plot of aligned angular momentum i_x vs rotational frequency ω for the ground-state and gamma-vibrational bands in ^{164}Dy. Harris parameters of $\mathcal{J}_0 = 40.6$ and $\mathcal{J}_1 = 114.2$, based on a fit to the lowest six transitions in the ground-state band, were used to calculate the reference.

TABLE IV. Matrix elements in eb used in the Coulex calculations: $M(E2)$'s between states in the ground band.

	0^+	2^+	4^+	6^+	8^+	10^+	12^+	14^+
0^+		2.3660						
2^+	2.3660	-2.8279	3.7940					
4^+		3.7940	-3.6175	4.7855				
6^+			4.7855	-4.3040	5.5990			
8^+				5.5990	-4.9033	6.3067		
10^+					6.3067	-5.4398	6.9420	
12^+						6.9420	-5.9293	7.5234
14^+							7.5234	-6.3821

at an energy of 1216 keV. The 762 keV and 689 keV lines are also clearly visible in a spectrum created by gating on the 1216 keV line. This transition is almost certainly a decay from a known state with an excitation energy of 1979 keV, reported in (n,γ) studies [18,25]. The reduced intensity of primary gammas from the neutron capture indicates that this state is an unresolved doublet with $J^\pi = (2^+,3^+),(2^+,3^+,4^+)$.

The spectrum shown in Fig. 7 can be used to determine an upper limit for the excitation strength of a hypothetical two-phonon state, assuming the decay to the one-phonon state occurs in the given energy range. A very small "peak," consisting of just 10 counts, occurs in the spectrum at an energy of 731 keV. We take this to be the lower limit of our ability to distinguish peaks in the spectrum. We assume a value of $B(E2;2^+_\gamma \rightarrow 4^+_{\gamma\gamma})$ = 1210 e^2 fm^4 for the excitation of the two-phonon state, based on a simple vibration-rotation model and the known $B(E2)$ values for transitions in the ground-state band. The Winther-deBoer Coulomb excitation code, using as input the matrix elements given in Tables IV, V, and VI, gives a yield for the $4^+_{\gamma\gamma} \rightarrow 2^+_\gamma$ transition that is 17 times greater than that of the $4^+_\gamma \rightarrow 2^+_\gamma$ transition. The measured strength of the 154 keV $4^+_\gamma \rightarrow 2^+_\gamma$ peak in the spectrum is 29 counts. Thus, we would expect to see a peak at 731 keV with approximately 250 counts when detector efficiency is taken into account. Therefore our assumption that 10 counts constitutes the smallest identifiable peak gives us an upper limit of 50 e^2 fm^4 or just 1 W.u.

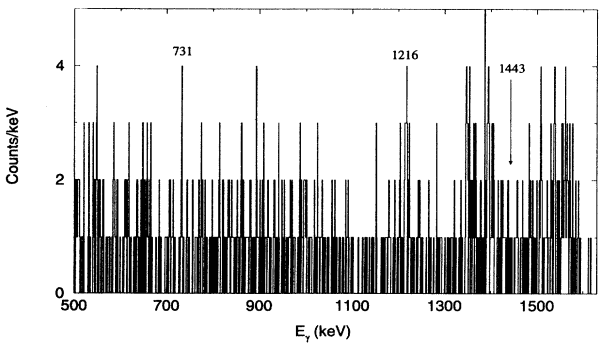

FIG. 7. A spectrum created by gating on the 762.4 and 688.9 keV transitions, which depopulate the 2^+_γ state. A $4^+_{\gamma\gamma} \rightarrow 2^+_\gamma$ transition in the energy range shown would correspond to an anharmonicity in the range $1.7 \leq E(4^+_{\gamma\gamma})/E(2^+_\gamma) \leq 3.1$.

It should be noted that the calculations used to determine decay strengths in the foregoing analysis do not include magnetic dipole transitions; this might lead to inaccuracies in the predicted branching ratios. It was found that for gamma-band to ground-band transistions the calculations overestimate the strength of the $I \rightarrow I-2$ transitions by about 40%. If we assume the same is true for transitions between the two-phonon and one-phonon gamma-vibrational bands, our upper limit for the excitation of the two-phonon state is 70 e^2 fm^4. This is significantly lower than the value 140 e^2 fm^4 found for the lower limit of $B(E2;4^+_{\gamma\gamma} \rightarrow 2^+_\gamma)$ in ^{168}Er [8], and less than would be expected for a collective transition.

Recently, a previously known 4^+ state at an energy of 2205 keV has been identified as a likely candidate for the two-phonon vibrational state in ^{164}Dy, corresponding to an anharmonicity of 2.9 [26]. The $4^+_{\gamma\gamma} \rightarrow 2^+_\gamma$ transition in this case would have an energy of 1443 keV. For this experiment, this energy lies within the range in which there are also Doppler-shifted coincidences with the $2^+ \rightarrow 0^+$ transition in ^{58}Ni. However, in the spectrum shown in Fig. 7, it is clear that there is no peak at 1443 keV. Using the same reasoning as above, the Coulomb excitation code gives a yield for a $4^+_{\gamma\gamma} \rightarrow 2^+_\gamma$ transition at this energy that is 7.5 times greater than that of the $4^+_\gamma \rightarrow 2^+_\gamma$ transition, corresponding to an expected peak size of 60 counts. If we again take ten counts as the lower limit of a statistically significant peak, this leads to an upper limit of 200 e^2 fm^4, or 4 W.u., for the strength of the proposed two-phonon to one-phonon transition. This limit does not rule out a collective two-phonon to one-phonon transition.

TABLE V. Matrix elements in eb used in the Coulex calculations: $M(E2)$'s between states in the ground band and states in the gamma vibrational bands.

	2^+_γ	3^+_γ	4^+_γ	5^+_γ	6^+_γ
0^+	-0.3480				
2^+	-0.4159	0.5502	-0.3602		
4^+	-0.0930	0.3480	-0.6182	0.6510	-0.3926
6^+			-0.1817	0.4922	-0.7566
8^+					-0.2461

TABLE VI. Matrix elements in eb used in the Coulex calculations: $M(E2)$'s between states in the gamma vibrational bands.

	2^+_γ	3^+_γ	4^+_γ	5^+_γ	6^+_γ	$4^+_{\gamma\gamma}$	$5^+_{\gamma\gamma}$	$6^+_{\gamma\gamma}$	$7^+_{\gamma\gamma}$	$8^+_{\gamma\gamma}$
2^+_γ	2.8279	3.7410	2.4490			-0.7782				
3^+_γ	-3.7410		3.6654	3.4287		0.5823	-0.7132			
4^+_γ	2.4490	-3.6654	-1.4470	3.4287	4.1351	-0.3448	0.7132	-0.6800		
5^+_γ		3.4287	-3.4287	-2.3841	3.1994	0.1556	-0.4959	0.7892	-0.6627	
6^+_γ			4.1351	-3.1994	-3.0743	-0.0469	0.2496	-0.6067	0.8448	-0.6544
$4^+_{\gamma\gamma}$	-0.7782	-0.5823	-0.3448	-0.1556	-0.0469	5.0645	4.4892	2.1401		
$5^+_{\gamma\gamma}$		-0.7132	-0.7132	-0.4959	-0.2496	-4.4892	2.3841	5.0587	3.1859	
$6^+_{\gamma\gamma}$			-0.6800	-0.7892	-0.6067	2.1401	-5.0587	0.6148	5.1372	3.9792
$7^+_{\gamma\gamma}$				-0.6627	-0.8448		3.1859	-5.1372	-0.6590	5.0587
$8^+_{\gamma\gamma}$					-0.6544			3.9792	-5.0587	-1.6344

Based on the results of these measurements, we conclude that there is no collective decay to the gamma-vibrational band in ^{164}Dy with anharmonicity less than 2.7, but that such a decay with greater anharmonicity cannot be ruled out by the present experiment. Hopefully, further experimental and theoretical research in this area will elucidate the nature of two-phonon excitations in rare-earth nuclei.

ACKNOWLEDGMENTS

Discussions with Prof. J.X. Saladin are gratefully acknowledged. The authors would also like to acknowledge the assistance of the HHIRF staff. Oak Ridge National Laboratory is managed for the U.S. Department of Energy by Martin Marietta Energy Systems under Contract No. DE-AC05-84OR21400.

[1] M. Sakai, At. Data Nucl. Data Tables **31**, 399 (1984).
[2] C. Baktash, J.X. Saladin, J. O'Brien, I.Y. Lee, and J.E. Holden, Phys. Rev. C **10**, 2265 (1974).
[3] V.G. Soloviev, Z. Phys. A **324**, 393 (1986).
[4] R. Piepenbring and M.K. Jammari, Nucl. Phys. **A481**, 81 (1988).
[5] M.K. Jammari and R. Piepenbring, Nucl. Phys. **A487**, 77 (1988).
[6] A. Charvet, R. Chery, R. Duffait, M. Morgue, and J. Sau, Nucl. Phys. **A213**, 117 (1973).
[7] W.F. Davidson, D.D. Warner, R.F. Casten, K. Schreckenbach, H.G. Borner, J. Simic, M. Stojanovic, M. Bogdanovic, S. Koicki, W. Gelletly, G.B. Orr, and M.L. Stelts, J. Phys. G **7**, 455 (1981).
[8] H.G. Borner, J. Jolie, S.J. Robinson, B. Krusche, P. Piepenbring, R.F. Casten, A. Aprahamian, and J.P. Draayer, Phys. Rev. Lett. **66**, 691 (1991).
[9] M. Oshima, T. Morikawa, H. Kusakari, N. Kobayashi, M. Sugawara, Y.H. Zhang, A. Ferragut, S. Ichikawa, N. Shinohara, Y. Nagame, M. Shibata, Y. Gono, and T. Inamura, Nucl. Phys. **A557**, 635c (1993).
[10] X. Wu, A. Aprahamian, S. Fischer, W. Reviol, G. Liu, and J.X. Saladin, Bull. Am. Phys. Soc. **37**, 997 (1992), and private communication.
[11] W. Korten, T. Härtlein, J. Gerl, D. Habs, and D. Schwalm, Phys. Lett. B **317**, 19 (1993).
[12] A. Winther and J. de Boer, in *Coulomb Excitation*, edited by K. Alder and A. Winther (Academic Press, New York, 1966).
[13] R.N. Oehlberg, L.L. Riedinger, A.E. Rainis, A.G. Schmidt, E.G. Funk, and J.W. Mihelich, Nucl. Phys. **A219**, 543 (1974).
[14] F. Kearns, G. Varley, G.D. Dracoulis, T. Inamura, J.C. Lisle, and J.C. Wilmott, Nucl. Phys. **A278**, 109 (1977).
[15] H.R. Hooper, J.M. Davidson, P.W. Green, D.M. Sheppard, and G.C. Neilson, Phys. Rev. C **15**, 1665 (1977).
[16] F.K. McGowan and W.T. Milner, Phys. Rev. C **23**, 1926 (1981).
[17] C.E. Doran, A.E. Stuchbery, H.H. Bolotin, A.P. Byrne, and G.J. Lampard, Phys. Rev. C **40**, 2035 (1989).
[18] E.N. Shurshikov, Nucl. Data Sheets **47**, 433 (1986).
[19] M. Oshima, H. Kusakari, M. Sugawara, T. Inamura, A. Hashizume, H. Kumagai, S. Ichikawa, and H. Iimura, RIKEN Accel. Prog. Rep. **24**, 21 (1990).
[20] H.J. Rose and D.M. Brink, Rev. Mod. Phys. **39**, 306 (1967).
[21] P.O. Lipas, Nucl. Phys. **39**, 468 (1962).
[22] L.L. Riedinger, N.R. Johnson, and J.H. Hamilton, Phys. Rev. **179**, 1214 (1969).
[23] R. Bengtsson, S. Frauendorf, and F.-R. May, At. Data Nucl. Data Tables **35**, 15 (1986).
[24] D.R. Bès, P. Federman, E. Maqueda, and A. Zucker, Nucl. Phys. **65**, 1 (1965).
[25] D.D. Warner, R.F. Casten, W.R. Kane, and W. Gelletly, Phys. Rev. C **27**, 2292 (1983).
[26] A. Aprahamian, Bull. Am. Phys. Soc. **38**, 1029 (1993).